Journal of Alzheimer's Disease 75 (2020) 1003–1016
DOI 10.3233/JAD-190954
IOS Press

In vivo MRI Structural and PET Metabolic Connectivity Study of Dopamine Pathways in Alzheimer's Disease

Leonardo Iaccarino[a,b,c,1], Arianna Sala[a,b,1], Silvia Paola Caminiti[a,b,1], Luca Presotto[b,d] and Daniela Perani[a,b,d,*] for the Alzheimer's Disease Neuroimaging Initiative[2]
[a]*Vita-Salute San Raffaele University, Milan, Italy*
[b]*In vivo Human Molecular and Structural Neuroimaging Unit, Division of Neuroscience, IRCCS San Raffaele Scientific Institute, Milan, Italy*
[c]*Memory and Aging Center, Weill Institute for Neurosciences, University of California San Francisco, San Francisco, CA, USA*
[d]*Nuclear Medicine Unit, San Raffaele Hospital, Milan, Italy*

Handling Associate Editor: Annalena Venneri

Accepted 24 March 2020

Abstract.
Background: Alzheimer's disease (AD) is characterized by an involvement of brain dopamine (DA) circuitry, the presence of which has been associated with emergence of both neuropsychiatric symptoms and cognitive deficits.
Objective: In order to investigate whether and how the DA pathways are involved in the pathophysiology of AD, we assessed by *in vivo* neuroimaging the structural and metabolic alterations of subcortical and cortical DA pathways and targets.
Methods: We included 54 healthy control participants, 53 amyloid-positive subjects with mild cognitive impairment due to AD (MCI-AD), and 60 amyloid-positive patients with probable dementia due to AD (ADD), all with structural 3T MRI and ^{18}F-FDG-PET scans. We assessed MRI-based gray matter reductions in the MCI-AD and ADD groups within an anatomical *a priori*-defined *Nigrostriatal* and *Mesocorticolimbic* DA pathways, followed by ^{18}F-FDG-PET metabolic connectivity analyses to evaluate network-level metabolic connectivity changes.
Results: We found significant tissue loss in the *Mesocorticolimbic* over the *Nigrostriatal* pathway. Atrophy was evident in the ventral striatum, orbitofrontal cortex, and medial temporal lobe structures, and already plateaued in the MCI-AD stage. Degree of atrophy in *Mesocorticolimbic* regions positively correlated with the severity of depression, anxiety, and apathy in MCI-AD and ADD subgroups. Additionally, we observed significant alterations of metabolic connectivity between the ventral striatum and fronto-cingulate regions in ADD, but not in MCI-AD. There were no metabolic connectivity changes within the *Nigrostriatal* pathway.
Conclusion: Our cross-sectional data support a clinically-meaningful, yet stage-dependent, involvement of the *Mesocorticolimbic* system in AD. Longitudinal and clinical correlation studies are needed to further establish the relevance of DA system involvement in AD.

Keywords: Alzheimer's disease, connectivity, dementia, dopamine systems, mild cognitive impairment, ventro-tegmental area

[1]These authors contributed equally to this work.

[2]Data used in preparation of this article were obtained from the Alzheimer's Disease Neuroimaging Initiative (ADNI) database (http://adni.loni.usc.edu). As such, the investigators within the ADNI contributed to the design and implementation of ADNI and/or provided data but did not participate in analysis or writing of this report. A complete listing of ADNI investigators can be found at: http://adni.loni.usc.edu/wp-content/uploads/how_to_apply/ADNI_Acknowledgement_List.pdf

*Correspondence to: Prof. Daniela Perani, MD, Vita-Salute San Raffaele University, Division of Neuroscience, IRCCS San Raffaele Scientific Institute, Nuclear Medicine Unit, IRCCS San Raffaele Hospital, Via Olgettina 60, Milan, Italy. Tel.: +39 02 264 2224; E-mail: perani.daniela@hsr.it.

INTRODUCTION

Alzheimer's disease (AD) is pathologically characterized by brain accumulation of amyloid-β (Aβ) plaques, neurofibrillary tau tangles, and neurodegeneration [1]. AD is further characterized by the progressive involvement of subcortical neuronal population [2], which produces neurochemical alterations in cholinergic and monoaminergic circuitry [3]. The evidence of a dopaminergic neurotransmission deficit in AD dates back to pioneering postmortem studies, reporting mild histological abnormalities in dopaminergic brainstem nuclei [4], and decreased levels of dopamine (DA), levodopa, and DA metabolites in subcortical and cortical dopaminergic targets [5]. In the nineties, molecular *in vivo* imaging studies based on positron emission tomography (PET) reported decreased post-synaptic DA receptor expression, particularly D2-like receptor, as well as a reduced transporter activity and expression of tyrosine hydroxylase levels in the major target of the ventro-tegmental area (VTA), i.e., the ventral striatum (VST) of AD patients [6–9]. The role of DA systems degeneration in AD pathogenesis has recently gained a renewed interest [10]. Animal studies suggested that neurons of the dopaminergic VTA might be especially vulnerable in AD (for a review, see [11]). Notably, VTA dopaminergic neurons project diffusely to both subcortical and cortical regions [12], innervating; 1) the VST, via the mesolimbic route [13]; 2) the medial fronto-cingulate cortex and orbitofrontal cortex, via the mesocortical route [14, 15]; 3) the medial temporal lobe structures, via the meso-hippocampal route [16]; 4) the amygdala, via the meso-amygdaloid route [10]. These widespread subcortical and cortical VTA projections jointly constitute the *Mesocorticolimbic* DA system, the dysregulation of which has been also associated with emergence of neuropsychiatric symptoms in AD [17, 18].

So far, few structural and functional magnetic resonance imaging (MRI) studies have assessed the alterations of the *Mesocorticolimbic* system in AD [19, 20]. These studies have shown significant associations between atrophy in VTA and medial temporal lobe, and cognitive performance in the AD clinical spectrum [19], as well as clinical stage-dependent disconnections within the VTA functional network, showing differences between mild cognitive impairment due to AD (MCI-AD) and dementia due to AD (ADD) [20]. These studies focused on the assessment of neurodegeneration and functional connectivity of the VTA, a small region, with limitations arising from the limited spatial resolution of the adopted neuroimaging techniques. It remains to be determined whether the dopaminergic routes projecting from the VTA are equally vulnerable, i.e., whether subcortical and cortical dopaminergic VTA targets are differentially affected in AD. Additionally, it is not yet fully understood whether VTA projections (i.e., *Mesocorticolimbic pathway)* are particularly vulnerable in AD compared to substantia nigra (SN) projections (i.e., *Nigrostriatal pathway*).

Here, with a multimodal neuroimaging approach, i.e. combining structural MRI and ^{18}F-FDG-PET brain metabolic data, we aim to provide a thorough assessment of the alterations in morphology and network topology characterizing the DA *Mesocorticolimbic* and *Nigrostriatal* pathway projections, addressing cross-sectionally the prodromal MCI-AD and ADD phases. We hypothesized that alterations of the DA *Mesocorticolimbic* pathway are present in AD since the earliest disease phases, and possibly associate with neuropsychiatric symptoms. Network measures were estimated with ^{18}F-FDG-PET brain glucose utilization data, employing an emerging methodological approach estimating metabolic connectivity [21]. ^{18}F-FDG-PET data provide crucial information about directionality of brain signaling, since increases in local metabolism reflect an increase in afferent effective connectivity [22]. This approach is based on the assumption that brain energy consumption is influenced by multiple pathological events, including altered neurotransmission [21, 22], and on the evidence of a significant coupling between neurotransmission impairment and integrity of metabolic networks [24].

Our group has previously shown that this approach successfully allows detection of metabolic connectivity alterations within the DA *Mesocorticolimbic and Nigrostriatal* systems, in both Parkinson's disease [25] and dementia with Lewy bodies [26].

METHODS

Participants

We retrospectively selected N = 60 patients with ADD, N = 53 subjects with MCI-AD, and N = 54 cognitively-normal healthy control subjects (HC) from the ADNI database (http://adni.loni.usc.edu). The ADNI was launched in 2003 as a public-private partnership, led by Principal Investigator Michael W. Weiner, MD. The primary goal of ADNI has been

to test whether serial MRI, PET, other biological markers, and clinical and neuropsychological assessment can be combined to measure the progression of MCI and early ADD. For up-to-date information, see http://www.adni-info.org. All procedures performed in studies involving the ADNI participants were carried out in accordance with the Helsinki declaration. The ADNI study was approved by the Institutional Review Boards of all of the participating institutions. Informed written consent was obtained from all participants and their legal representatives at each site prior to the collection of clinical, genetic, and imaging data.

We included only subjects with both MRI scan performed on a 3T scanner and ^{18}F-FDG-PET scan, cognitive and neuropsychiatric evaluations available and performed within 6 months. As in the ADNI1 study MRI scans were acquired on a 1.5T scanner, subjects/patients enrolled in the ADNI1 study were excluded, hence resulting in a sample limited to ADNIGO and ADNI2 cohorts. As for clinical protocol, ADD patients were enrolled based on NINCDS/ADRDA criteria for probable AD [27]; MCI subjects were enrolled based on evidence of memory impairment and in the absence of significant impairment in other cognitive domains, thus representing amnestic single domain MCI cases (see clinical protocols on http://adni.loni.usc.edu/). Since ADNI enrollment criteria are based on the 1984 NINCDS/ADRDA clinical criteria for AD [27], known to yield some mismatch against definite neuropathological diagnosis [28], we set additional and more stringent inclusion criteria to select our clinical sample. Specifically, an additional inclusion criterion was the availability of an amyloid ^{18}F-Florbetapir-PET scan to establish presence of cerebral fibrillary amyloid-β plaques [29]. We thus selected only MCI-AD subjects and ADD patients with available neuroimaging biomarkers indicating a high likelihood of underlying AD etiology [30, 31], i.e., 1) amyloid positive at ^{18}F-Florbetapir-PET [30, 31], also in accordance with the current research framework for AD [1], and 2) presenting evidence of neuronal injury, as determined by ^{18}F-FDG-PET (i.e., temporal-parietal/precuneus hypometabolism) [30, 31]. Amyloid positivity was determined based on semi-quantification of ^{18}F-Florbetapir-PET images, using a validated cut-off of $SUVR_{CEREBELLUM}>1.11$, as detailed elsewhere [32, 33]. Presence of an AD-like hypometabolism pattern at ^{18}F-FDG-PET was determined based on an optimized SPM-based procedure, extensively described elsewhere [34], allowing accurate detection of disease-specific hypometabolism patterns not only in cases with overt dementia [34–38] but also in prodromal disease phases [34, 37–40]. As biomarker of neuronal injury, we selected ^{18}F-FDG-PET hypometabolism over MRI atrophy due to the higher accuracy reported for ^{18}F-FDG-PET hypometabolism in identifying ADD patients [average ^{18}F-FDG-PET sensitivity: 0.84, specificity 0.86; average MRI sensitivity: 0.81, specificity 0.75] and predicting progression to ADD in MCI subjects [average ^{18}F-FDG-PET sensitivity: 0.74, specificity 0.76; average MRI sensitivity: 0.73, specificity 0.62], as compared to MRI [41]. This was also done in light of the recent evidence suggesting that MRI hippocampal atrophy might not be a specific marker for AD, as it is also observed in non-AD syndromes with amnestic presentations [42], differently from ^{18}F-FDG-PET AD-like hypometabolism [43]. As for controls, we selected only healthy individuals lacking evidence of underlying neurodegenerative processes at ^{18}F-FDG-PET, based on the well-established association between hypometabolism topographies and neurodegenerative conditions [34, 44] and following from the evidence that an ^{18}F-FDG-PET scan negative for neurodegeneration significantly predicts clinical stability in healthy controls [40]. A demographic summary of the study groups is available in Table 1.

Global cognitive and neuropsychiatric evaluations

We relied on Mini-Mental State Examination (MMSE) [45] and Clinical Dementia Rating (CDR) [46] questionnaires to provide a measure of global cognitive status also supporting MCI and dementia clinical diagnosis in the included clinical groups.

Given that we were specifically interested in testing whether alterations of the DA *Mesocorticolimbic* pathway were associated with presence of neuropsychiatric symptoms, we also considered the Neuropsychiatric Inventory (NPI) [47], so as to obtain a standardized measure of severity/frequency of a wide range of neuropsychiatric symptoms in our clinical groups. The NPI questionnaire is composed of 12 sub-items addressing delusions, hallucinations, agitation/aggression, dysphoria/depression, anxiety, euphoria/elation, apathy/indifference, disinhibition, irritability, aberrant motor behavior, night-time sleep disturbances, and appetite/eating changes. The maximum total score ($a \times b$) obtainable from each

Table 1
Demographic and clinical features

	ADD	MCI-AD	HC	p
Sample size	60	53	54	-
Sex (f/m)	31/29	19/34	27/27	0.190
Age (y)	73.04 ± 7.75	72.01 ± 7.73	73.36 ± 5.98	0.601
Education (y)	15.63 ± 2.67	16.4 ± 2.75	16.31 ± 2.68	0.253
MMSE	22.63 ± 2.41	27.02 ± 1.9	28.91 ± 1.34	1.07e-38[#]
CDR	0.81 ± 0.29	0.52 ± 0.14	0.03 ± 0.15	1.42e-44[#]
NPI - Total	7.27 ± 8.54	5.06 ± 6.02	1.09 ± 3.5	5.97e-06[§]
NPI - Delusions	0.33 ± 1.37	0.18 ± 0.93	0 ± 0	0.200
NPI - Hallucinations	0.12 ± 0.42	0.12 ± 0.52	0 ± 0	0.190
NPI - Agitation/Aggression	0.47 ± 1.44	0.61 ± 1.25	0.21 ± 0.86	0.240
NPI - Dysphoria/Depression	0.57 ± 0.96	0.65 ± 1.35	0.06 ± 0.23	0.000[§]
NPI - Anxiety	0.57 ± 1.24	0.78 ± 1.91	0.13 ± 0.56	0.040[°]
NPI - Euphoria/Elation	0.65 ± 1.35	0.57 ± 1.24	0.43 ± 0.99	0.530
NPI - Apathy/Indifference	1.55 ± 2.37	0.51 ± 1.46	0.49 ± 1.36	0.000[¥]
NPI - Disinhibition	0.37 ± 1.34	0.33 ± 1.67	0 ± 0	0.230
NPI - Irritability	0.92 ± 1.94	0.49 ± 1.17	0.25 ± 0.87	0.040*
NPI - Aberrant Motor Behavior	0.48 ± 1.26	0.16 ± 0.88	0.02 ± 0.14	0.020*
NPI - Night-time Sleep Disturbances	0.5 ± 1.35	0.67 ± 1.89	0.25 ± 0.98	0.330
NPI - Appetite/Eating Changes	1.27 ± 2.69	0.53 ± 1.8	0.15 ± 1.1	0.010*

Table showing demographic summary plus baseline biomarker and clinical data. ADD, dementia due to Alzheimer's disease; CDR, Clinical Dementia Rating; HC, healthy controls; MCI-AD, mild cognitive impairment due to Alzheimer's disease; MMSE, Mini-Mental State Examination; NPI, Neuropsychiatric Inventory. [§]ADD>HC, MCI-AD>HC; [#]ADD<HC, MCI-AD<HC, ADD<MCI-AD; [°]MCI-AD>HC; *AD>HC; [¥]ADD>MCI-AD, AD>HC. All results were corrected for multiple comparisons with the Bonferroni correction.

neuropsychiatric symptoms sub-item is 12 and the NPI total cumulative score is 144 [47].

Differences across the three groups in demographic, cognitive, and neuropsychiatric data were assessed with an Analysis of Variance (ANOVA), by applying a Bonferroni-type adjustment for multiple comparisons.

MRI pre-processing

Structural MRI (3 Tesla T1-weighted MPRAGE sequence) were downloaded from the ADNI database. Diffeomorphic Anatomical Registration Through Exponentiated Lie Algebra (DARTEL) was used to generate a study-specific template by aligning the gray and white matter images nonlinearly to a common space. DARTEL procedure consisted in three steps: 1) tissue segmentation of the T1 images for each subject using the segmentation tool of SPM12; 2) construction of a study-specific template of each tissue type in MNI space; 3) non-linear transformation estimation necessary to warp grey and white matter images to match the study-specific template.

An explicit mask for subsequent voxel-level analysis was created by averaging the smoothed, warped, and modulate gray matter segmented maps of the healthy controls, to be then thresholded at >0.1.

Voxel-level atrophy W-score maps estimation

To create maps of statistical deviation of brain volume from the reference control group, we estimated voxel-level atrophy W-score maps [48, 49]. Briefly, w-scores are computed by subtracting, for each individual and each voxel, the measured value with the expected value considering the mean of the healthy controls and nuisance factors, then dividing by the standard deviation of the residuals, according to the following formula:

$$\text{W - score} = \frac{\left[\begin{array}{c}\text{(patient's raw value)} - \\ \text{(value expected in the control group for the patient's age sex and TBV)}\end{array}\right]}{\text{SD of the residuals in controls.}}$$

A detailed description of the W-score approach in neuroimaging analysis is available in [48, 49]. W-scores in the control group have a normal z-like distribution (mean = 0; standard deviation = 1) and thus patients' W-score maps at the voxel-level show where each voxel value per patient would fall and whether the deviation would be significant or not. W-score atrophy maps were calculated considering the effect of age, sex, and total brain volume (TBV; gray

matter + white matter volume), in order to investigate regional effects relative to global atrophy/shrinkage.

Regions-of-interest definition

In order to reconstruct the anatomical neurotransmitter pathways, regions of interest (ROIs) delineating the *Mesocorticolimbic* (VTA-based) and *Nigrostriatal* (SN-based) DA targets were selected according to previous literature [15, 50], following a similar methodological approach adopted in previous studies [25, 26]. The *Nigrostriatal* DA pathway was included as a "control" pathway, for comparison only. More specifically, we selected for the *Nigrostriatal* pathway: the middle/superior frontal gyri, the supplementary motor cortex, the medial segment of the postcentral gyrus, the medial segment of the precentral gyrus, and the medial segment of the superior frontal gyri. For the *Mesocorticolimbic* pathway, we selected: the entorhinal area, the hippocampus, the amygdala, the parahippocampal gyrus, the medial orbitofrontal cortex, the lateral orbitofrontal cortex, the subcallosal area, the orbital part of the inferior frontal gyrus, the medial frontal cortex, and the anterior/middle cingulate gyri.

Additionally, the dorsal striatum and VST ROIs were created by splitting caudate and putamen ROIs on the axial plane taking the anterior commissure/posterior commissure line as reference. All the ROIs were bilateral and provided by Neuromorphometrics Inc. (http://www.neuromorphometrics.com/), under academic subscription. The selection resulted in a total of N = 19 ROIs, of which N = 12 ROIs for the *Mesocorticolimbic* DA pathway and N = 7 ROIs for the *Nigrostriatal* DA pathway.

Gray matter reductions at the regional level

Regional gray matter reductions were estimated by first extracting regional atrophy W-scores from the above-mentioned ROIs and for all the groups, with the REX toolbox for SPM (http://web.mit.edu/swg/software.htm). Lower W-scores indicated more severe regional atrophy compared to HC. W-scores, corrected for age, sex, and TBV, were then compared across the three groups with a multivariate analysis of covariance (MANCOVA). The resulting statistical models were deemed significant at $p < 0.05$ Bonferroni corrected for multiple comparisons. Bonferroni correction was applied for *post-hoc* analysis.

In order to better characterize the clinical significance of these findings, we investigated the relationship between NPI measures (when clinically relevant, i.e., significantly affected in our patients' cohorts) and grey matter reductions in the pathological cohort (ADD and MCI-AD) by means of non-parametric Spearman correlations. We selected a non-parametric test as NPI scores follow a non-continuous distribution [51].

^{18}F-FDG-PET pre-processing

^{18}F-FDG-PET images were downloaded from the ADNI database and were co-registered to their respective structural MRI scan in the native space with SPM12 (https://www.fil.ion.ucl.ac.uk/spm/software/spm12/). Then, warping parameters obtained through the DARTEL spatial normalization were applied to the co-registered ^{18}F-FDG-PET images, which were subsequently smoothed with an 8 mm^3 Gaussian filter. This step limits statistical noise and bias due to inter-subject anatomical differences, thus increasing statistical power [52, 53].

After warping and smoothing ^{18}F-FDG-PET images were respectively scaled to their cerebral global mean (CGM), in order to account for between-subject and between-scan uptake variability [54]. This method has been shown to yield higher signal-to-noise ratio compared to the choice of other references regions [55], that might be affected by a number of factors, including cerebrovascular disease (e.g., [56]), brain trauma (e.g., [57]), or aging (e.g., [58]). This procedure provided warped, smoothed $SUVR_{CGM}$ ^{18}F-FDG-PET images.

Metabolic connectivity analysis in Mesocorticolimbic and Nigrostriatal pathways

To evaluate the association among regional metabolism within the DA pathways, we tested the correlation between each possible pairwise ROIs combination considering the effect of all the remaining *Mesocorticolimbic* network regions. Regional metabolism was estimated by first extracting the average regional ^{18}F-FDG-PET $SUVR_{CGM}$ from the above-mentioned ROIs and for all the groups, with REX toolbox for SPM. We then ran a partial correlation model, separately for HC and symptomatic groups (MCI-AD and ADD). Additionally, correlation coefficients resulting for each pairwise combination were tested for difference among groups by means of a z-test, considering age and gender as nuisance variables. Results are reported at a relatively liberal threshold ($p < 0.01$) as well as following cor-

Table 2
ROI-level gray matter reductions

Regions	System	F	Partial η^2	p	ADD<HC	MCI-AD< HC	ADD< MCI-AD
Hippocampus	**M**	48.00	0.37	**0.000**	**0.000**	**0.000**	0.161
Parahippocampal Gyrus	**M**	40.29	0.33	**0.000**	**0.000**	**0.000**	0.097
Entorhinal Area	**M**	35.53	0.30	**0.000**	**0.000**	**0.000**	**0.046**
Amygdala	**M**	28.77	0.26	**0.000**	**0.000**	**0.000**	0.106
Medial Orbital Gyrus	**M**	18.27	0.18	**0.000**	**0.000**	**0.000**	1.00
Middle Frontal Gyrus	**N**	12.25	0.13	**0.000**	**0.000**	**0.001**	1.00
Orbital Part of Inferior Frontal Gyrus	**M**	9.88	0.11	**0.000**	**0.008**	**0.020**	1.00
Ventral Striatum	**M**	8.78	0.10	**0.000**	**0.001**	**0.002**	1.00
Precentral Gyrus Medial Segment	**N**	7.07	0.08	**0.001**	**0.002**	**0.011**	1.00

Table showing regions with significant gray matter reductions across the three clinical groups. The statistical threshold was set at $p < 0.05$ Bonferroni corrected for multiple comparisons. Regions are sorted according to decreasing effect size, as measured by Partial-Eta squared. The MCI-AD<CN, ADD<HC and ADD<MCI-AD columns show the *p*-values of *post-hoc* tests, Bonferroni corrected (see Methods). ADD, Alzheimer's disease dementia; MCI-AD, mild cognitive impairment due to Alzheimer's disease; HC, healthy controls; M, mesocorticolimbic; N, nigrostriatal.

rection for multiple comparisons using Bonferroni correction ($p < 0.05$).

RESULTS

Demographics and clinical/neuropsychiatric evaluation

The included participants did not differ in terms of sex ($p = 0.190$), age ($p = 0.601$), and education ($p = 0.253$) (Table 1). As expected, MMSE and CDR scores showed that global cognitive status was significantly, and progressively, deteriorated in MCI-AD and ADD (Table 1). Both symptomatic groups showed higher NPI total and depression scores compared to HC (NPI – Total, MCI-AD $p = 0.006$, ADD $p < 0.001$; NPI - Dysphoria/Depression, MCI-AD ($p = 0.006$, ADD $p = 0.02$). At Bonferroni *post-hoc* comparison, MCI-AD group showed significantly higher NPI scores than HC for one item, i.e., anxiety ($p = 0.043$), whereas ADD group showed higher scores than HC in Apathy/Indifference ($p < 0.001$), Irritability ($p = 0.042$), Aberrant Motor Behavior ($p = 0.022$), and Appetite/Eating Changes ($p = 0.011$) (Table 1). At last follow-up visit, 33 out of 53 (62.3%) MCI-AD converted to ADD.

Gray matter reductions at the regional level

Nine out of the total 19 selected regions of interest showed significant gray matter volume reductions in MCI-AD and ADD patients, with the net majority (77.7%) involving structures belonging to the *Mesocorticolimbic* DA pathway. Regions in the *Mesocorticolimbic* DA pathway indeed presented the most significant differences between patients and HC, with 58.3% of VTA targets presenting significant gray matter reductions (see Table 2 and detailed effect sizes therein). Ventral striatum, orbitofrontal cortex, and medial temporal lobe structures, namely hippocampus, parahippocampal gyrus, entorhinal area, and amygdala, showed the peaking gray matter reductions, with most of the effect already detectable at the MCI-AD stage (see Fig. 1).

Considering the *Nigrostriatal* pathway regions, grey matter reductions involved only 28.57% of the SN targets, and limited to the middle frontal gyrus and precentral gyrus medial segment, in both MCI-AD and ADD in comparison with HC, whereas subcortical structures showed no differences (Fig. 1). Severity of grey matter reductions in these regions was relatively mild, as suggested by the small effect sizes (0.08–0.13) (Table 2).

When testing the correlation between NPI measures and grey matter reductions in the *Mesocorticolimbic* regions, we found that NPI depression sub-scale score correlated with atrophy in the medial orbitofrontal cortex ($R_s = -0.22$, $p = 0.004$); NPI anxiety sub-scale score with atrophy in the ventral striatum ($R_s = -0.22$; $p = 0.004$); NPI apathy sub-scale score with atrophy in the hippocampus ($R_s = -0.26$; $p = 0.001$), parahippocampal gyrus ($R_s = -0.24$; $p = 0.002$), entorhinal area ($R_s = -0.25$; $p = 0.001$), and amygdala ($R_s = -0.25$; $p = 0.001$). In all aforementioned *Mesocorticolimbic* regions, higher NPI scores were associated with more severe atrophy in both the symptomatic groups (MCI-AD and ADD). All reported correlations survived Bonferroni-correction for multiple comparisons.

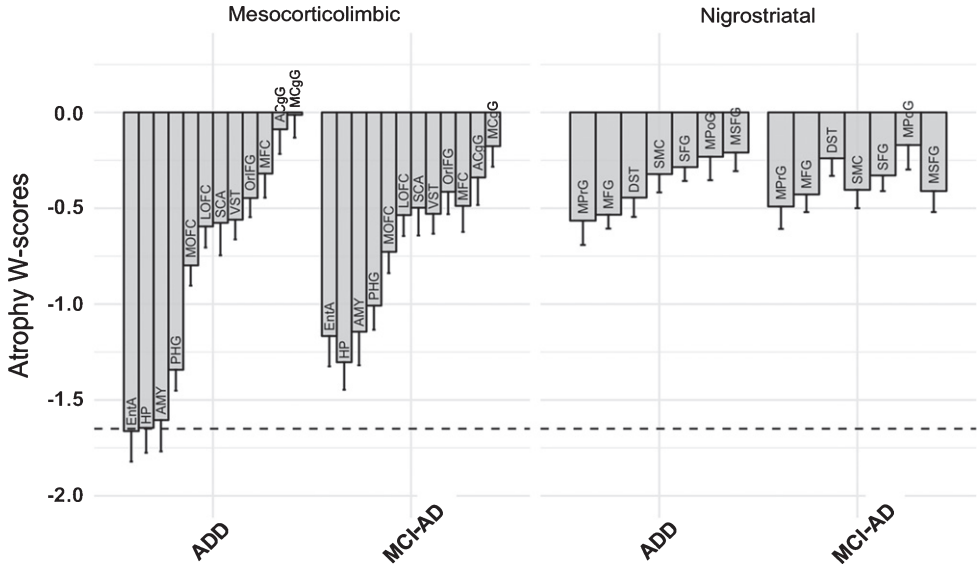

Fig. 1. Box plot showing atrophic regions as expressed by W-score values, obtained from the comparison of patients with healthy control group in the *Mesocorticolimbic* and *Nigrostriatal* DA pathways. The horizontal dashed line represents a threshold for significance ($W < -1.64$, $p < 0.05$). ACgG, anterior cingulate gyrus; ADD, Alzheimer's disease dementia; AMY, amygdala; DST, dorsal striatum; EntA, entorhinal area; HP, the hippocampus; LOFC, the lateral orbitofrontal cortex; MCgG, the middle cingulate gyri; MCI-AD, mild cognitive impairment due to Alzheimer's disease; MFC, medial frontal cortex; MFG, the middle frontal gyrus; MOFC, medial orbitofrontal cortex; MPoG, the medial segment of the postcentral gyrus; MPrG, the medial segment of the precentral gyrus; MSFG, the medial segment of the superior frontal gyrus; OrIFG, the orbital part of the inferior frontal gyrus; SCA, the subcallosal area; PHG, parahippocampal gyrus; SFG, the superior frontal gyri; SMC, the supplementary motor cortex; VST, ventral striatum.

Metabolic connectivity analysis

Regions belonging to the *Mesocorticolimbic* pathway showed significant metabolic connectivity alterations in ADD (threshold, $p < 0.01$ uncorrected for multiple comparisons). These changes specifically involved 1) multiple VST functional connections, including those to frontal and cingulate regions, i.e., middle cingulate gyrus, lateral orbitofrontal cortex, and orbital part of the inferior frontal gyrus; 2) the parahippocampal gyri connections with medial temporal lobe structures, including the amygdala, the entorhinal cortex, and the hippocampus; and 3) the lateral orbitofrontal connections with the anterior cingulate gyrus. The finding of significant metabolic connectivity alterations between the VST and middle cingulate gyrus and between the VST and lateral orbitofrontal cortex, was also confirmed after Bonferroni correction for multiple comparisons ($p = 0.04$ and $p = 0.05$, respectively, see Fig. 2). The MCI-AD group showed a more limited connectivity reconfiguration, with the only significant (liberal threshold, $p < 0.01$ uncorrected for multiple comparisons) alteration between orbital part of the inferior frontal gyrus and the middle cingulate cortex, not surviving, however, Bonferroni correction for multiple comparisons at $p < 0.05$ (Fig. 2).

In the ADD group, the *Nigrostriatal* pathway showed no significant metabolic connectivity alterations. The dorsal striatum, main hub of the *Nigrostriatal* system, was well connected with the other *Nigrostriatal* nodes, in both MCI-AD and ADD groups.

DISCUSSION

This cross-sectional study explores the structural alterations and metabolic connectivity changes in the DA *Mesocorticolimbic* and *Nigrostriatal* systems in subjects with MCI and dementia due to AD. Within the *Mesocorticolimbic* DA system, we showed that both MCI-AD and ADD patients had significant tissue loss not only in memory-related medial temporal lobe regions, as expected, but also in other major VTA targets, notably the VST and the orbito-frontal cortices. Regions belonging to the *Nigrostriatal* pathway exhibited overall less pronounced alterations, with significant gray matter reductions limited to the middle frontal gyri and precentral gyrus medial seg-

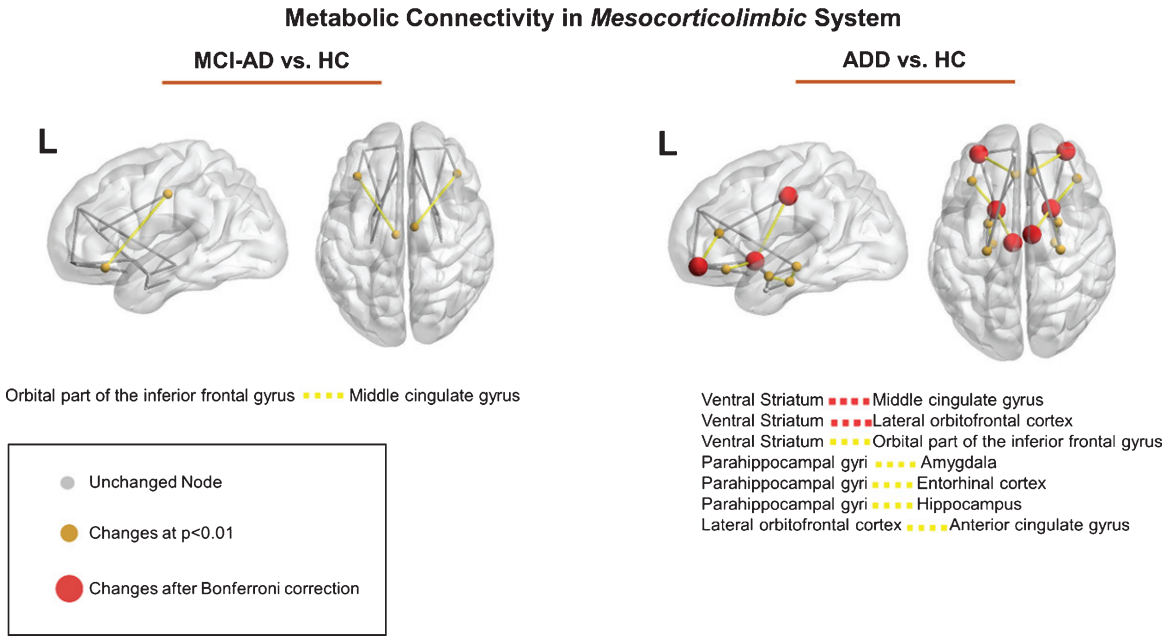

Fig. 2. Metabolic connectivity analysis of the *Mesocorticolimbic* pathway. Figure represents metabolic connectivity changes obtained when comparing partial correlation coefficients between MCI-AD versus HC and ADD versus HC. Yellow edges represent significant metabolic connectivity changes, with ochre nodes for p-values thresholded at $p < 0.01$, uncorrected for multiple comparison and red nodes for connectivity changes surviving Bonferroni correction for multiple comparisons ($p < 0.05$). Metabolic connectivity changes are listed below each brain render; only significant metabolic connectivity changes at $p < 0.01$, uncorrected for multiple comparisons (yellow dotted lines) and at $p < 0.05$, Bonferroni-corrected for multiple comparisons (red dotted lines) are reported. Brain renderings were obtained using BrainNet [99]. ADD, Alzheimer's disease dementia; HC, healthy controls, MCI-AD, mild cognitive impairment due to Alzheimer's disease.

ment, but no changes in the basal ganglia structures. Metabolic connectivity analyses revealed significant functional changes in the VST connections to the fronto-cingulate regions, but only in the dementia stage. Our data overall provide evidence for a significant, yet phase-dependent, structural and metabolic involvement of regions belonging to the *Mesocorticolimbic* pathway in AD [48]. Our finding of a more widespread loss of gray matter in regions innervated by the VTA, as compared to the SN, is consistent with recent evidence in animal models of AD, where selective degeneration of VTA neurons and impaired DA outflow to VTA targets, i.e., nucleus accumbens and hippocampus, were reported [11]. The factors underlying the more pronounced vulnerability of regions belonging to the *Mesocorticolimbic* over the *Nigrostriatal* pathway remain unclear. Recently, it has been suggested that the selective vulnerability of the VTA and its *Mesocorticolimbic* targets might be explained in the context of the cholinergic hypothesis for AD [10]. It has long been recognized that cholinergic projections from latero-dorsal and posterior peduncolo-pontine tegmental nuclei make selective synaptic contact with DA tyrosine hydroxylase-positive terminals in VTA [59], where they are critical modulators of dopaminergic activity [60, 61]. Building on this evidence, it is possible that selective vulnerability of the VTA DA neurons described in the literature [11], and of regions belonging to the *Mesocorticolimbic* pathway described here, might be at least partially ascribed to the progressive loss of cholinergic neurons characterizing AD [10].

This is the first study to adopt a dopaminergic framework to study atrophy and metabolic connectivity in AD, reporting that vulnerability of regions innervated by the VTA is not limited to targets of the mesolimbic/hippocampal route but extends to the orbitofrontal cortices (mesocortical route) and amygdala (meso-amygdaloid route) as well, suggesting a widespread vulnerability of the *Mesocorticolimbic* pathway. With the exception of the entorhinal area, atrophy of all the aforementioned brain regions already reached a peak in the MCI-AD group, with no further neurodegeneration in ADD (Table 2), pointing at an involvement of these regions in early disease phase.

Among the targets of VTA dopaminergic projections, the hippocampus showed the most pronounced

tissue loss in both MCI-AD and ADD cohorts. The hippocampal structures are known to be the locus of severe neurodegeneration in AD and MCI-AD [62], by accumulation of neurofibrillary tangles and diffuse amyloid load, and are the earliest and most severely affected brain regions in typical, late-onset AD [63]. Of note, while the ventral hippocampus receives massive dopaminergic projections from the VTA, the dense dopaminergic receptors in the dorsal hippocampus receive not only by VTA projections, but also by tyrosine hydroxylase-rich afferents from the locus coeruleus [64, 65]. The latter represents an early region of aggregation for AD pathology [66, 67], and thus the relevant role of the alterations of this dopaminergic input to the hippocampus and other cortical structures [68], particularly for the cognitive status [62], should be considered.

Additionally, our data show significant tissue loss in the other major mesolimbic target, i.e., ventral striatum, already in prodromal disease stages. Neurofibrillary tangles in the basal portions of the VST have been observed relatively early in the course of AD, already in Stage IV of Braak's classification, when deposits are mostly restricted to limbic brain regions only [69]. The VST has a higher density of neurofibrillary tangles than throughout the striatum in AD [70], which is consistent with our observation of a ventral *greater-than* dorsal gradient of atrophy and with other evidence showing a prevalent involvement of VST in AD pathology [71]. As mentioned in the introduction, both hippocampal formation and VST are innervated by VTA dopaminergic projections, the degeneration of which has been shown to produce lower DA outflow, equally affecting the hippocampus and VST in AD transgenic animal models [11]. We also found that amygdala, the major target of the meso-amygdaloid route, suffered significant gray matter loss in both our MCI-AD and ADD cohorts. Notably, DA is recognized a neuromodulator of both hippocampal and amygdala synaptic plasticity; the DA projections arising from the VTA to the dorsal hippocampus are a major determinant of memory encoding, via an enhancement of long-term potentiation and learning performance [72–74], whereas VTA DA input to the amygdala modulates consolidation of long-term memories [75]. Accordingly, restoration of DA transmission ameliorates memory and learning performances in mouse models of AD [11, 76, 77]. Last, we also found evidence for gray matter loss in cortical targets belonging to the mesocortical route, with significant atrophy in the medial orbitofrontal cortices and pars orbitalis of the inferior frontal gyrus, in both MCI-AD and ADD cases.

We found that severity of gray matter loss within regions belonging to the *Mesocorticolimbic* pathway was associated with greater severity of neuropsychiatric symptoms. Specifically, depression was linked to gray matter loss within the meso-cortical route, anxiety to gray matter loss within the mesolimbic route, and apathy to gray matter loss within the meso-hippocampal/meso-amygdaloid routes, suggesting that vulnerability of different *Mesocorticolimbic* targets is associated with specific neuropsychiatric signatures [78]. In this direction, multiple lines of evidence point at the clinical relevance of VTA degeneration (and of its targets) in both AD animal models [10] and humans [19, 20, 79, 80]. In humans, VTA and VST degeneration was associated with both neuropsychiatric symptoms [20, 79, 80] and memory/cognitive dysfunction [19] in MCI-AD and ADD patients. Furthermore, the severity of cognitive impairment in AD has been previously associated with shape abnormalities of the VST [81]. MRI atrophy in the VST was found in both early and more advanced AD stages [82, 83], and with an associated increased risk of clinical progression from MCI-AD to ADD during 2 years of follow-up (Hazard Ratio = 1.59, 95% Confidence Interval: 1.16 to 2.18) [83]. Although the cardinal symptom of typical, late-onset AD pathology is memory impairment, a high percentage of AD patients actually develops neuropsychiatric symptoms during the disease course [84]. Among the neuropsychiatric symptoms, depression and apathy are the most frequently reported symptoms in both MCI-AD subjects and ADD patients [84], and our cohort showed a similar neuropsychiatric profile (Table 1). Presence of neuropsychiatric symptoms is also associated, in cognitively healthy subjects, with an higher risk of developing MCI-AD, and, in MCI-AD subjects, with a higher likelihood of progression to dementia [85–87].

We investigated also metabolic connectivity changes between regions belonging to the *Mesocorticolimbic* pathway, using an emerging connectivity approach based on metabolic ^{18}F-FDG-PET data. So far, metabolic connectivity studies in AD have focused mainly on the investigation of metabolic connectivity alterations in resting-state brain networks [88–90], and on the modulation of metabolic connectivity by modifiable life factors [91–94]. Altogether, these studies have consistently shown that the default mode network is especially vulner-

able in AD [88–90, 95], with involvement of other large-scale networks in atypical clinical presentation [88]. Broadly, these results suggest a multi-factorial modulation of brain connectivity in AD (see [21, 96] for reviews). Here we adopted a different approach specifically aimed at assessing metabolic connectivity alterations in neurotransmission pathways. This novel approach has also been adopted in two previous studies, reporting metabolic connectivity alterations of the DA pathways in both Parkinson's disease and dementia with Lewy bodies [25, 26], at consistence with the well-known neurochemical imbalance reported in these conditions [21]. Recently, it has been demonstrated that the investigation of metabolic connectivity of the dopaminergic pathways, based on ^{18}F-FDG-PET, yields reliable information on the molecular architecture of dopaminergic pathways, and can provide comparable results to those based on ^{123}I-FP-CIT imaging [97]. Here, we found that most regions within the *Mesocorticolimbic* pathway showed a preserved functional connectivity in AD. Only in the ADD group, the VST showed metabolic connectivity alterations with the lateral part of orbito-frontal cortex and the middle cingulate gyrus. Notably, the VST represents a crucial hub within the *Mesocorticolimbic* system, with tight interconnections towards medial and lateral orbitofrontal cortices [50]. On the contrary, we did not observe alterations of the VST interconnections in the MCI-AD group, suggesting that connectivity changes within the *Mesocorticolimbic* network are a later phenomenon, likely following VST neural loss (already detectable in the MCI-AD group) in the AD pathologic cascade. The discrepancy between detected atrophy and metabolic connectivity observed in the MCI-AD phase requires further investigation. Still, it can be noted that the degree of gray matter loss was significant but not particularly severe in *Mesocorticolimbic* structures, ranging approximately from 0.5 to 1.5 standard deviations below the mean (depending on the ROIs; Fig. 1); additionally, it must be underlined that structural MRI and ^{18}F-FDG-PET measure related but partially independent aspects of neurodegeneration; as a prototypical example, although it is well-established that hippocampus shows significant gray matter loss in AD, it is also well-known that it does not show significant glucose metabolism reductions in AD maps [48]. Although the nature of the discrepancy between MRI and ^{18}F-FDG-PET findings is poorly understood, it is possible that synaptic compensatory mechanisms play a role [98]. Possibly, similar compensatory mechanisms might be at play also in the atrophied regions of the *Mesocorticolimbic* pathway that do not show alterations in metabolic connectivity in the MCI phase.

In conclusion, this study points at an involvement of the *Mesocorticolimbic* DA neuromodulatory system in AD, that seems stage-dependent, as emerging from both structural and molecular connectivity data from two groups in the AD continuum at different cognitive stages. Structural and metabolic connectivity alterations in the *Mesocorticolimbic* pathway in ADD is not limited to VST and hippocampus but encompasses other relevant dopaminergic targets, including the amygdala and the orbitofrontal cortex, with a comparable volume loss along symptomatic disease phases. The lack of metabolic connectivity alterations in MCI-AD suggests that functional changes within the *Mesocorticolimbic* pathway degeneration are likely to appear in more advanced disease stages, likely following more severe pathology spreading. Molecular PET studies based on radiotracers specific for DA neurotransmission are necessary to definitely demonstrate that dopaminergic neurotransmission impairment is at the basis of the structural and metabolic changes here observed in crucial DA *Mesocorticolimbic* targets. Longitudinal prospective studies, at difference with the present cross-sectional evidence, are also needed to establish the diagnostic and prognostic relevance of DA system involvement in AD pathogenesis.

ACKNOWLEDGMENTS

This work was supported by the Italian Ministry of Health (Ricerca Finalizzata Progetto Reti Nazionale AD NET-2011-02346784).

Data collection and sharing for this project was also funded by the Alzheimer's Disease Neuroimaging Initiative (ADNI) (National Institutes of Health Grant U01 AG024904) and DOD ADNI (Department of Defense award number W81XWH-12-2-0012). ADNI is funded by the National Institute on Aging, the National Institute of Biomedical Imaging and Bioengineering, and through generous contributions from the following: AbbVie, Alzheimer's Association; Alzheimer's Drug Discovery Foundation; Araclon Biotech; BioClinica, Inc.; Biogen; Bristol-Myers Squibb Company; CereSpir, Inc.; Cogstate; Eisai Inc.; Elan Pharmaceuticals, Inc.; Eli Lilly and Company; EuroImmun; F. Hoffmann-La Roche Ltd and its affiliated company Genentech, Inc.; Fujirebio; GE Healthcare; IXICO Ltd.; Janssen Alzheimer

Immunotherapy Research & Development, LLC.; Johnson & Johnson Pharmaceutical Research & Development LLC.; Lumosity; Lundbeck; Merck & Co., Inc.; Meso Scale Diagnostics, LLC.; NeuroRx Research; Neurotrack Technologies; Novartis Pharmaceuticals Corporation; Pfizer Inc.; Piramal Imaging; Servier; Takeda Pharmaceutical Company; and Transition Therapeutics. The Canadian Institutes of Health Research is providing funds to support ADNI clinical sites in Canada. Private sector contributions are facilitated by the Foundation for the National Institutes of Health (http://www.fnih.org). The grantee organization is the Northern California Institute for Research and Education, and the study is coordinated by the Alzheimer's Therapeutic Research Institute at the University of Southern California. ADNI data are disseminated by the Laboratory for Neuro Imaging at the University of Southern California.

Authors' disclosures available online (https://www.j-alz.com/manuscript-disclosures/19-0954r2).

REFERENCES

[1] Jack CRJ, Bennett DA, Blennow K, Carrillo MC, Dunn B, Haeberlein SB, Holtzman DM, Jagust W, Jessen F, Karlawish J, Liu E, Molinuevo JL, Montine T, Phelps C, Rankin KP, Rowe CC, Scheltens P, Siemers E, Snyder HM, Sperling R, Contributors (2018) NIA-AA Research Framework: Toward a biological definition of Alzheimer's disease. *Alzheimers Dement* **14**, 535-562.

[2] Wenk GL (2003) Neuropathologic changes in Alzheimer's disease. *J Clin Psychiatry* **64**, 7-10.

[3] Trillo L, Das D, Hsieh W, Medina B, Moghadam S, Lin B, Dang V, Sanchez MM, De Miguel Z, Ashford JW (2013) Ascending monoaminergic systems alterations in Alzheimer's disease. Translating basic science into clinical care. *Neurosci Biobehav Rev* **37**, 1363-1379.

[4] Gibb WR, Mountjoy CQ, Mann DM, Lees AJ (1989) The substantia nigra and ventral tegmental area in Alzheimer's disease and Down's syndrome. *J Neurol Neurosurg Psychiatry* **52**, 193-200.

[5] Storga D, Vrecko K, Birkmayer JGD, Reibnegger G (1996) Monoaminergic neurotransmitters, their precursors and metabolites in brains of Alzheimer patients. *Neurosci Lett* **203**, 29-32.

[6] Rinne JO, Säkö E, Paljärvi L, Mölsä PK, Rinne UK (1986) Brain dopamine D-1 receptors in senile dementia. *J Neurol Sci* **73**, 219-230.

[7] Allard P, Alafuzoff I, Carlsson A, Eriksson K, Ericson E, Gottfries C-G, Marcusson JO (1990) Loss of dopamine uptake sites labeled with [3H] GBR-12935 in Alzheimer's disease. *Eur Neurol* **30**, 181-185.

[8] Murray AM, Weihmueller FB, Marshall JF, Hurtig HI, Gottleib GL, Joyce JN (1995) Damage to dopamine systems differs between Parkinson's disease and Alzheimer's disease with parkinsonism. *Ann Neurol* **37**, 300-312.

[9] Joyce JN, Smutzer G, Whitty CJ, Myers A, Bannon MJ (1997) Differential modification of dopamine transporter and tyrosine hydroxylase mRNAs in midbrain of subjects with Parkinson's, Alzheimer's with parkinsonism, and Alzheimer's disease. *Mov Disord* **12**, 885-897.

[10] D'Amelio M, Puglisi-Allegra S, Mercuri N (2018) The role of dopaminergic midbrain in Alzheimer's disease: Translating basic science into clinical practice. *Pharmacol Res* **130**, 414-419.

[11] Nobili A, Latagliata EC, Viscomi MT, Cavallucci V, Cutuli D, Giacovazzo G, Krashia P, Rizzo FR, Marino R, Federici M, De Bartolo P, Aversa D, Dell'Acqua MC, Cordella A, Sancandi M, Keller F, Petrosini L, Puglisi-Allegra S, Mercuri NB, Coccurello R, Berretta N, D'Amelio M (2017) Dopamine neuronal loss contributes to memory and reward dysfunction in a model of Alzheimer's disease. *Nat Commun* **8**, 14727.

[12] Bjorklund A, Dunnett SB (2007) Dopamine neuron systems in the brain: An update. *Trends Neurosci* **30**, 194-202.

[13] Le Moal M, Simon H (1991) Mesocorticolimbic dopaminergic network: Functional and regulatory roles. *Physiol Rev* **71**, 155-234.

[14] Chau BKH, Jarvis H, Law C-K, Chong TT-J (2018) Dopamine and reward: A view from the prefrontal cortex. *Behav Pharmacol* **29**, 569-583.

[15] Oades RD, Halliday GM (1987) Ventral tegmental (A10) system: Neurobiology. 1. Anatomy and connectivity. *Brain Res Rev* **12**, 117-165.

[16] Ntamati NR, Lüscher C (2016) VTA projection neurons releasing GABA and glutamate in the dentate gyrus. *Eneuro* **3**, ENEURO.0137-16.2016.

[17] Lanari A, Amenta F, Silvestrelli G, Tomassoni D, Parnetti L (2006) Neurotransmitter deficits in behavioural and psychological symptoms of Alzheimer's disease. *Mech Ageing Dev* **127**, 158-165.

[18] Mitchell RA, Herrmann N, Lanctôt KL (2011) The role of dopamine in symptoms and treatment of apathy in Alzheimer's disease. *CNS Neurosci Ther* **17**, 411-427.

[19] De Marco M, Venneri A (2018) Volume and connectivity of the ventral tegmental area are linked to neurocognitive signatures of Alzheimer's disease in humans. *J Alzheimers Dis* **63**, 1-14.

[20] Serra L, D'Amelio M, Di Domenico C, Dipasquale O, Marra C, Mercuri NB, Caltagirone C, Cercignani M, Bozzali M (2018) In vivo mapping of brainstem nuclei functional connectivity disruption in Alzheimer's disease. *Neurobiol Aging* **72**, 72-82.

[21] Sala A, Perani D (2019) Brain molecular connectivity in neurodegenerative diseases: Recent advances and new perspectives using positron emission tomography. *Front Neurosci* **13**, 617.

[22] Riedl V, Utz L, Castrillón G, Grimmer T, Rauschecker JP, Ploner M, Friston KJ, Drzezga A, Sorg C (2016) Metabolic connectivity mapping reveals effective connectivity in the resting human brain. *Proc Natl Acad Sci U S A* **113**, 428-433.

[23] Perani D (2014) FDG-PET and amyloid-PET imaging: The diverging paths. *Curr Opin Neurol* **27**, 405-413.

[24] Holtbernd F, Ma Y, Peng S, Schwartz F, Timmermann L, Kracht L, Fink GR, Tang CC, Eidelberg D, Eggers C (2015) Dopaminergic correlates of metabolic network activity in Parkinson's disease. *Hum Brain Mapp* **36**, 3575-3585.

[25] Sala A, Caminiti SP, Presotto L, Premi E, Pilotto A, Cosseddu M, Paghera B, Borroni B (2017) Altered brain metabolic connectivity at multiscale level in early Parkinson's disease. *Sci Rep* **7**, 4256.

[26] Caminiti SP, Tettamanti M, Sala A, Presotto L, Iannaccone S, Cappa SF, Magnani G, Perani D (2017) Metabolic con-

nectomics targeting brain pathology in dementia with Lewy bodies. *J Cereb Blood Flow Metab* **37**, 1311-1325.

[27] McKhann G, Drachman D, Folstein M, Katzman R, Price D, Stadlan EM (1984) Clinical diagnosis of Alzheimer's disease: Report of the NINCDS-ADRDA Work Group under the auspices of Department of Health and Human Services Task Force on Alzheimer's Disease. *Neurology* **34**, 939-944.

[28] Beach TG, Monsell SE, Phillips LE, Kukull W (2012) Accuracy of the clinical diagnosis of Alzheimer disease at National Institute on Aging Alzheimer Disease Centers, 2005-2010. *J Neuropathol Exp Neurol* **71**, 266-273.

[29] Clark CM, Schneider JA, Bedell BJ, Beach TG, Bilker WB, Mintun MA, Pontecorvo MJ, Hefti F, Carpenter AP, Flitter ML, Krautkramer MJ, Kung HF, Coleman RE, Doraiswamy PM, Fleisher AS, Sabbagh MN, Sadowsky CH, Reiman PEM, Zehntner SP, Skovronsky DM; AV45-A07 Study Group (2011) Use of florbetapir-PET for imaging β-amyloid pathology. *JAMA* **305**, 275-283.

[30] McKhann GM, Knopman DS, Chertkow H, Hyman BT, Jack Jr CR, Kawas CH, Klunk WE, Koroshetz WJ, Manly JJ, Mayeux R (2011) The diagnosis of dementia due to Alzheimer's disease: Recommendations from the National Institute on Aging-Alzheimer's Association workgroups on diagnostic guidelines for Alzheimer's disease. *Alzheimers Dement* **7**, 263-269.

[31] Albert MS, DeKosky ST, Dickson D, Dubois B, Feldman HH, Fox NC, Gamst A, Holtzman DM, Jagust WJ, Petersen RC, Snyder PJ, Carrillo MC, Thies B, Phelps CH (2011) The diagnosis of mild cognitive impairment due to Alzheimer's disease: Recommendations from the National Institute on Aging-Alzheimer's Association workgroups on diagnostic guidelines for Alzheimer's disease. *Alzheimers Dement* **7**, 270-279.

[32] Landau SM, Mintun MA, Joshi AD, Koeppe RA, Petersen RC, Aisen PS, Weiner MW, Jagust WJ (2012) Amyloid deposition, hypometabolism, and longitudinal cognitive decline. *Ann Neurol* **72**, 578-586.

[33] Joshi AD, Pontecorvo MJ, Clark CM, Carpenter AP, Jennings DL, Sadowsky CH, Adler LP, Kovnat KD, Seibyl JP, Arora A, Saha K, Burns JD, Lowrey MJ, Mintun MA, Skovronsky DM (2012) Performance characteristics of amyloid PET with florbetapir F 18 in patients with Alzheimer's disease and cognitively normal subjects. *J Nucl Med* **53**, 378-384.

[34] Perani D, Della Rosa PA, Cerami C, Gallivanone F, Fallanca F, Vanoli EG, Panzacchi A, Nobili F, Pappatà S, Marcone A, Garibotto V, Castiglioni I, Magnani G, Cappa SF, Gianolli L (2014) Validation of an optimized SPM procedure for FDG-PET in dementia diagnosis in a clinical setting. *Neuroimage Clin* **6**, 445-54.

[35] Caminiti SP, Alongi P, Majno L, Volontè MA, Cerami C, Gianolli L, Comi G, Perani D (2017) Evaluation of an optimized [18F]fluoro-deoxy-glucose positron emission tomography voxel-wise method to early support differential diagnosis in atypical Parkinsonian disorders. *Eur J Neurol* **24**, 687-e26.

[36] Cerami C, Dodich A, Greco L, Iannaccone S, Magnani G, Marcone A, Pelagallo E, Santangelo R, Cappa SF, Perani D (2016) The role of single-subject brain metabolic patterns in the early differential diagnosis of primary progressive aphasias and in prediction of progression to dementia. *J Alzheimers Dis* **55**, 183-197.

[37] Perani D, Cerami C, Caminiti SP, Santangelo R, Coppi E, Ferrari L, Pinto P, Passerini G, Falini A, Iannaccone S, Cappa SF, Comi G, Gianolli L, Magnani G (2016) Cross-validation of biomarkers for the early differential diagnosis and prognosis of dementia in a clinical setting. *Eur J Nucl Med Mol Imaging* **43**, 499-508.

[38] Caminiti SP, Sala A, Iaccarino L, Beretta L, Pilotto A, Gianolli L, Iannaccone S, Magnani G, Padovani A, Ferini-Strambi L, Perani D (2019) Brain glucose metabolism in Lewy body dementia: Implications for diagnostic criteria. *Alzheimers Res Ther* **11**, 20.

[39] Cerami C, Della Rosa PA, Magnani G, Santangelo R, Marcone A, Cappa SF, Perani D (2015) Brain metabolic maps in mild cognitive impairment predict heterogeneity of progression to dementia. *Neuroimage Clin* **7**, 187-194.

[40] Iaccarino L, Sala A, Perani D (2019) Predicting long-term clinical stability in amyloid-positive subjects by FDG-PET. *Ann Clin Transl Neurol* **6**, 1113-1120.

[41] Frisoni GB, Bocchetta M, Chételat G, Rabinovici GD, De Leon MJ, Kaye J, Reiman EM, Scheltens P, Barkhof F, Black SE, Brooks DJ, Carrillo MC, Fox NC, Herholz K, Nordberg A, Jack CR, Jagust WJ, Johnson KA, Rowe CC, Sperling RA, Thies W, Wahlund LO, Weiner MW, Pasqualetti P, DeCarli C (2013) Imaging markers for Alzheimer disease: Which vs how. *Neurology* **81**, 487-500.

[42] Nelson PT, Dickson DW, Trojanowski JQ, Jack CR, Boyle PA, Arfanakis K, Rademakers R, Alafuzoff I, Attems J, Brayne C, Coyle-Gilchrist ITS, Chui HC, Fardo DW, Flanagan ME, Halliday G, Hokkanen SRK, Hunter S, Jicha GA, Katsumata Y, Kawas CH, Keene CD, Kovacs GG, Kukull WA, Levey AI, Makkinejad N, Montine TJ, Murayama S, Murray ME, Nag S, Rissman RA, Seeley WW, Sperling RA, White CL, Yu L, Schneider JA (2019) Limbic-predominant age-related TDP-43 encephalopathy (LATE): Consensus working group report. *Brain* **142**, 1503-1527.

[43] Cerami C, Dodich A, Iannaccone S, Magnani G, Santangelo R, Presotto L, Marcone A, Gianolli L, Cappa SF, Perani D (2018) A biomarker study in long-lasting amnestic mild cognitive impairment. *Alzheimer Res Ther* **10**, 42.

[44] Iaccarino L, Sala A, Caminiti SP, Perani D (2017) The emerging role of PET imaging in dementia. *F1000Research* **6**, 1830.

[45] Teng EL, Chui HC (1987) The Modified Mini-Mental State (3MS) examination. *J Clin Psychiatry* **48**, 314-318.

[46] Morris JC (1993) The Clinical Dementia Rating (CDR): Current version and scoring rules. *Neurology* **43**, 2412-2414.

[47] Cummings JL, Mega M, Gray K, Rosenberg-Thompson S, Carusi DA, Gornbein J (1994) The Neuropsychiatric Inventory: Comprehensive assessment of psychopathology in dementia. *Neurology* **44**, 2308.

[48] La Joie R, Perrotin A, Barré L, Hommet C, Mézenge F, Ibazizene M, Camus V, Abbas A, Landeau B, Guilloteau D, de La Sayette V, Eustache F, Desgranges B, Chételat G (2012) Region-specific hierarchy between atrophy, hypometabolism, and 2-amyloid (Aβ) load in Alzheimer's disease dementia. *J Neurosci* **32**, 16265-16273.

[49] Ossenkoppele R, Cohn-Sheehy BI, La Joie R, Vogel JW, Möller C, Lehmann M, van Berckel BNM, Seeley WW, Pijnenburg YA, Gorno-Tempini ML (2015) Atrophy patterns in early clinical stages across distinct phenotypes of Alzheimer's disease. *Hum Brain Mapp* **36**, 4421-4437.

[50] Tziortzi AC, Haber SN, Searle GE, Tsoumpas C, Long CJ, Shotbolt P, Douaud G, Jbabdi S, Behrens TEJ, Rabiner EA, Jenkinson M, Gunn RN (2013) Connectivity-based functional analysis of dopamine release in the striatum using diffusion-weighted MRI and positron emission tomography. *Cereb Cortex* **24**, 1165-1177.

[51] Lai CKY (2014) The merits and problems of Neuropsychiatric Inventory as an assessment tool in people with dementia and other neurological disorders. *Clin Interv Aging* **9**, 1051.
[52] Friston K (2002) Beyond phrenology: What can neuroimaging tell us about distributed circuitry? *Annu Rev Neurosci* **25**, 221-250.
[53] Presotto L, Ballarini T, Caminiti SP, Bettinardi V, Gianolli L, Perani D (2017) Validation of 18F-FDG-PET single-subject optimized SPM procedure with different PET scanners. *Neuroinformatics* **15**, 151-163.
[54] Gallivanone F, Della Rosa PA, Perani D, Gilardi MC, Castiglioni I (2017) The impact of different 18FDG PET healthy subject scans for comparison with single patient in SPM analysis. *Q J Nucl Med Mol Imaging* **61**, 115-132.
[55] Dukart J, Mueller K, Horstmann A, Vogt B, Frisch S, Barthel H, Becker G, M??ller HE, Villringer A, Sabri O, Schroeter ML (2010) Differential effects of global and cerebellar normalization on detection and differentiation of dementia in FDG-PET studies. *Neuroimage* **49**, 1490-1495.
[56] Zheng L, Vinters H V, Mack WJ, Weiner MW, Chui HC, project IVD program (2016) Differential effects of ischemic vascular disease and Alzheimer's disease on brain atrophy and cognition. *J Cereb Blood Flow Metab* **36**, 204-215.
[57] McKee AC, Stein TD, Kiernan PT, Alvarez VE (2015) The neuropathology of chronic traumatic encephalopathy. *Brain Pathol* **25**, 350-364.
[58] Giorgio A, Santelli L, Tomassini V, Bosnell R, Smith S, De Stefano N, Johansen-Berg H (2010) Age-related changes in grey and white matter structure throughout adulthood. *Neuroimage* **51**, 943-951.
[59] Smiley JF, Mesulam M-M (1999) Cholinergic neurons of the nucleus basalis of Meynert receive cholinergic, catecholaminergic and GABAergic synapses: An electron microscopic investigation in the monkey. *Neuroscience* **88**, 241-255.
[60] Yeomans JS (1995) Role of tegmental cholinergic neurons in dopaminergic activation, antimuscarinic psychosis and schizophrenia. *Neuropsychopharmacology* **12**, 3.
[61] Yeomans J, Baptista M (1997) Both nicotinic and muscarinic receptors in ventral tegmental area contribute to brain-stimulation reward. *Pharmacol Biochem Behav* **57**, 915-921.
[62] Shi F, Liu B, Zhou Y, Yu C, Jiang T (2009) Hippocampal volume and asymmetry in mild cognitive impairment and Alzheimer's disease: Metap-analyses of MRI studies. *Hippocampus* **19**, 1055-1064.
[63] Pini L, Pievani M, Bocchetta M, Altomare D, Bosco P, Cavedo E, Galluzzi S, Marizzoni M, Frisoni GB (2016) Brain atrophy in Alzheimer's disease and aging. *Ageing Res Rev* **30**, 25-48.
[64] Kempadoo KA, Mosharov E V., Choi SJ, Sulzer D, Kandel ER (2016) Dopamine release from the locus coeruleus to the dorsal hippocampus promotes spatial learning and memory. *Proc Natl Acad Sci U S A* **113**, 14835-14840.
[65] Takeuchi T, Duszkiewicz AJ, Sonneborn A, Spooner PA, Yamasaki M, Watanabe M, Smith CC, Fernández G, Deisseroth K, Greene RW, Morris RGM (2016) Locus coeruleus and dopaminergic consolidation of everyday memory. *Nature* **537**, 357-362.
[66] Braak H, Alafuzoff I, Arzberger T, Kretzschmar H, Tredici K (2006) Staging of Alzheimer disease-associated neurofibrillary pathology using paraffin sections and immunocytochemistry. *Acta Neuropathol* **112**, 389-404.
[67] Theofilas P, Ehrenberg AJ, Dunlop S, Di Lorenzo Alho AT, Nguy A, Leite REP, Rodriguez RD, Mejia MB, Suemoto CK, Ferretti-Rebustini REDL, Polichiso L, Nascimento CF, Seeley WW, Nitrini R, Pasqualucci CA, Jacob Filho W, Rueb U, Neuhaus J, Heinsen H, Grinberg LT (2017) Locus coeruleus volume and cell population changes during Alzheimer's disease progression: A stereological study in human postmortem brains with potential implication for early-stage biomarker discovery. *Alzheimers Dement* **13**, 236-246.
[68] Devoto P, Flore G (2006) On the origin of cortical dopamine: Is it a co-transmitter in noradrenergic neurons? *Curr Neuropharmacol* **4**, 115-125.
[69] Braak H, Braak E (1991) Neuropathological stageing of Alzheimer-related changes. *Acta Neuropathol* **82**, 239-259.
[70] Engelhardt E, Laks J (2008) Alzheimer disease neuropathology: Understanding autonomic dysfunction. *Dement Neuropsychol* **2**, 183-191.
[71] Martorana A, Koch G (2014) Is dopamine involved in Alzheimer's disease? *Front Aging Neurosci* **6**, 252.
[72] McNamara CG, Tejero-Cantero Á, Trouche S, Campo-Urriza N, Dupret D (2014) Dopaminergic neurons promote hippocampal reactivation and spatial memory persistence. *Nat Neurosci* **17**, 1658.
[73] Broussard JI, Yang K, Levine AT, Tsetsenis T, Jenson D, Cao F, Garcia I, Arenkiel BR, Zhou F-M, De Biasi M (2016) Dopamine regulates aversive contextual learning and associated in vivo synaptic plasticity in the hippocampus. *Cell Rep* **14**, 1930-1939.
[74] Lisman JE, Grace AA (2005) The hippocampal-VTA loop: Controlling the entry of information into long-term memory. *Neuron* **46**, 703-713.
[75] Rossato JI, Radiske A, Kohler CA, Gonzalez C, Bevilaqua LR, Medina JH, Cammarota M (2013) Consolidation of object recognition memory requires simultaneous activation of dopamine D1/D5 receptors in the amygdala and medial prefrontal cortex but not in the hippocampus. *Neurobiol Learn Mem* **106**, 66-70.
[76] Ambrée O, Richter H, Sachser N, Lewejohann L, Dere E, de Souza Silva MA, Herring A, Keyvani K, Paulus W, Schäbitz W-R (2009) Levodopa ameliorates learning and memory deficits in a murine model of Alzheimer's disease. *Neurobiol Aging* **30**, 1192-1204.
[77] Guzmán-Ramos K, Moreno-Castilla P, Castro-Cruz M, McGaugh JL, Martínez-Coria H, LaFerla FM, Bermúdez-Rattoni F (2012) Restoration of dopamine release deficits during object recognition memory acquisition attenuates cognitive impairment in a triple transgenic mice model of Alzheimer's disease. *Learn Mem* **19**, 453-460.
[78] Lee GJ, Lu PH, Hua X, Lee S, Wu S, Nguyen K, Teng E, Leow AD, Jack Jr CR, Toga AW (2012) Depressive symptoms in mild cognitive impairment predict greater atrophy in Alzheimer's disease-related regions. *Biol Psychiatry* **71**, 814-821.
[79] Mega MS, Lee L, Dinov ID, Mishkin F, Toga AW, Cummings JL (2000) Cerebral correlates of psychotic symptoms in Alzheimer's disease. *J Neurol Neurosurg Psychiatry* **69**, 167-171.
[80] Bruen PD, McGeown WJ, Shanks MF, Venneri A (2008) Neuroanatomical correlates of neuropsychiatric symptoms in Alzheimer's disease. *Brain* **131**, 2455-2463.
[81] de Jong LW, Ferrarini L, van der Grond J, Milles JR, Reiber JHC, Westendorp RGJ, Bollen ELEM, Middelkoop HAM,

van Buchem MA (2011) Shape abnormalities of the striatum in Alzheimer's disease. *J Alzheimers Dis* **23**, 49-59.

[82] Liu Y, Paajanen T, Zhang Y, Westman E, Wahlund L-O, Simmons A, Tunnard C, Sobow T, Mecocci P, Tsolaki M (2010) Analysis of regional MRI volumes and thicknesses as predictors of conversion from mild cognitive impairment to Alzheimer's disease. *Neurobiol Aging* **31**, 1375-1385.

[83] Yi H-A, Möller C, Dieleman N, Bouwman FH, Barkhof F, Scheltens P, van der Flier WM, Vrenken H (2016) Relation between subcortical grey matter atrophy and conversion from mild cognitive impairment to Alzheimer's disease. *J Neurol Neurosurg Psychiatry* **87**, 425-432.

[84] Lyketsos CG, Carrillo MC, Ryan JM, Khachaturian AS, Trzepacz P, Amatniek J, Cedarbaum J, Brashear R, Miller DS (2011) Neuropsychiatric symptoms in Alzheimer's disease. *Alzheimers Dement* **7**, 532-539.

[85] Geda YE, Roberts RO, Mielke MM, Knopman DS, Christianson TJH, Pankratz VS, Boeve BF, Sochor O, Tangalos EG, Petersen RC (2014) Baseline neuropsychiatric symptoms and the risk of incident mild cognitive impairment: A population-based study. *Am J Psychiatry* **171**, 572-581.

[86] Monastero R, Mangialasche F, Camarda C, Ercolani S, Camarda R (2009) A systematic review of neuropsychiatric symptoms in mild cognitive impairment. *J Alzheimers Dis* **18**, 11-30.

[87] Peters ME, Rosenberg PB, Steinberg M, Norton MC, Welsh-Bohmer KA, Hayden KM, Breitner J, Tschanz JT, Lyketsos CG, Investigators CC (2013) Neuropsychiatric symptoms as risk factors for progression from CIND to dementia: The Cache County Study. *Am J Geriatr Psychiatry* **21**, 1116-1124.

[88] Ballarini T, Iaccarino L, Magnani G, Ayakta N, Miller BL, Jagust WJ, Gorno-tempini ML, Rabinovici GD, Perani D, Francisco S (2016) Neuropsychiatric subsyndromes and brain metabolic network dysfunctions in early onset Alzheimer's disease. *Hum Brain Mapp* **37**, 4234-4247.

[89] Morbelli S, Drzezga A, Perneczky R, Frisoni GB, Caroli A, van Berckel BNM, Ossenkoppele R, Guedj E, Didic M, Brugnolo A, Sambuceti G, Pagani M, Salmon E, Nobili F (2012) Resting metabolic connectivity in prodromal Alzheimer's disease. A European Alzheimer Disease Consortium (EADC) project. *Neurobiol Aging* **33**, 2533-2550.

[90] Herholz K, Haense C, Gerhard A, Jones M, Anton-Rodriguez J, Segobin S, Snowden JS, Thompson JC, Kobylecki C (2017) Metabolic regional and network changes in Alzheimer's disease subtypes. *J Cereb Blood Flow Metab* **38**, 1796-1806.

[91] Morbelli S, Perneczky R, Drzezga A, Frisoni GB, Caroli A, van Berckel BNM, Ossenkoppele R, Guedj E, Didic M, Brugnolo A, Naseri M, Sambuceti G, Pagani M, Nobili F (2013) Metabolic networks underlying cognitive reserve in prodromal Alzheimer disease: A European Alzheimer disease consortium project. *J Nucl Med* **54**, 894-902.

[92] Malpetti M, Ballarini T, Presotto L, Garibotto V, Tettamanti M, Perani D (2017) Gender differences in healthy aging and Alzheimer's dementia: A 18F-FDG-PET study of brain and cognitive reserve. *Hum Brain Mapp* **38**, 4212-4227.

[93] Perani D, Farsad M, Ballarini T, Lubian F, Malpetti M, Fracchetti A (2017) The impact of bilingualism on brain reserve and metabolic connectivity in Alzheimer's dementia. *Proc Natl Acad Sci U S A* **114**, 1690-1695.

[94] Malpetti M, Sala A, Vanoli EG, Gianolli L, Luzi L, Perani D (2018) Unfavourable gender effect of high body mass index on brain metabolism and connectivity. *Sci Rep* **8**, 12584.

[95] Pagani MM, Giuliani A, Öberg J, De Carli F, Morbelli S, Girtler N, Bongioanni F, Arnaldi D, Accardo J, Bauckneht M, Chincarini A, Sambuceti G, Jonsson C, Nobili F (2017) Progressive disgregation of brain networking from normal aging to Alzheimer's disease. Independent component analysis on FDG-PET data. *J Nucl Med* **58**, 1132-1139.

[96] Yakushev I, Drzezga A, Habeck C (2017) Metabolic connectivity: Methods and applications. *Curr Opin Neurol* **30**, 677-685.

[97] Verger A, Horowitz T, Chawki MB, Eusebio A, Bordonne M, Azulay J-P, Girard N, Guedj E (2020) From metabolic connectivity to molecular connectivity: Application to dopaminergic pathways. *Eur J Nucl Med Mol Imaging* **47**, 413-424.

[98] Rodriguez-Oroz MC, Gago B, Clavero P, Delgado-Alvarado M, Garcia-Garcia D, Jimenez-Urbieta H (2015) The relationship between atrophy and hypometabolism: Is it regionally dependent in dementias? *Curr Neurol Neurosci Rep* **15**, 44.

[99] Xia M, Wang J, He Y (2013) BrainNet Viewer: A network visualization tool for human brain connectomics. *PLoS One* **8**, e68910.